Numerically Optimized Performance of Diabatic Distillation Columns

May 26, 2001

Markus Schaller and Karl Heinz Hoffmann
Institute of Physics, Chemnitz University of Technology
D-09107 Chemnitz, Germany

Gino Siragusa
Department of Chemistry
San Diego State University
San Diego, CA 92182-1030, USA

Peter Salamon
Department of Mathematical and Computer Sciences
San Diego State University
San Diego, CA 92182-7720, USA

Bjarne Andresen
Ørsted Laboratory, University of Copenhagen
Universitetsparken 5, DK-2100 Copenhagen Ø, Denmark

Abstract

Recently, the concept of equal thermodynamic distance (ETD) has been proposed to minimize entropy production in a distillation process using a diabatic column. ETD gives the optimal temperature profile to first-order in N^{-1}, where N is the number of trays. ETD however, does not in general give the true minimum for distillation columns with few trays. We therefore apply a fully numerical, multidimensional optimization routine to determine minimum entropy production. Since this method does not depend on an underlying theory we expect a true minimum to be revealed. We then compare the performance of ETD and numerical optimization by varying the number of trays and the purity requirements. Our results show surprisingly good agreement between the ETD results and the ones obtained numerically.

Keywords

Diabatic Distillation, Entropy Production, Equal Thermodynamic Distance, Optimization.

1 Introduction

Within the area of finite-time thermodynamics [1, 2] many papers have been devoted to minimizing entropy production in thermodynamic processes. In particular, the problem is well suited for studying potential exergy savings in a distillation process. The basic idea is a thermally controlled (diabatic) distillation column (see figure 1). Instead of just one heat source (reboiler) and one heat sink (condenser) a diabatic column uses a heat exchanger at each tray of the column. The idea goes back to the work of Z. Fonyo in the early seventies [3] but has recently been explored by a number of authors [4, 5, 6, 7, 8, 9, 10, 11]. The additional heat exchangers add or remove heat to maintain a particular temperature profile inside the column. The temperature profile prescribed by the theory of equal thermodynamic distance (ETD) achieves minimum entropy production for the separation process to lowest order in one over the number of trays[1]. The purpose of the present paper is to compare this asymptotically minimum entropy producing operation with the true minimum obtained numerically.

The concept of equal thermodynamic distance uses a thermodynamic metric based on the entropy state function of the mixture to be separated. The thermodynamic length $\mathcal{L}$ of a process is given by the line element [4]

$$d\mathcal{L} = \sqrt{-d\vec{\mathbf{Z}}^{\mathrm{t}}\, D^2 S\, d\vec{\mathbf{Z}}}\,, \tag{1}$$

where $\vec{\mathbf{Z}} = (U, V, \ldots)$ is the vector of extensive variables and D^2S is the matrix of partial derivatives $\partial^2 S/\partial Z_i \partial Z_j$. In section 3 the derivation of the ETD principle and its application to distillation will be presented.

2 The Distillation Model

The mixture to be separated is introduced as feed F usually near the middle of the column and the seperated components are removed at the top as distillate D and at the bottom as bottoms B. The column is considered to be operating at steady-state so all extensive quantities are per unit time. For convenience, only binary mixtures are considered and the pressure is assumed

[1] It is well known that any reasonable heat integration will aid in the reduction of entropy production [12], here we attempt to find the optimal heating profile.

to be constant throughout the column. In steady state operation, the feed, distillate and bottoms obey the flow balance equations

$$F = D + B \tag{2}$$

$$x_F F = x_D D + x_B B\,, \tag{3}$$

where x_F, x_B and x_D denote the corresponding mole fractions of the more volatile component (lower boiling point) in the liquid phase. Similarly, the amount of material flowing out of a tray must be equal to the amount of material flowing into a tray. Hence, vapor coming up from tray $n+1$ and liquid flowing down from tray n have to balance the distillate D above the feed and the bottoms B below the feed respectively (Figure 2),

$$V_{n+1} - L_n = \begin{cases} D & \text{above feed} \\ -B & \text{below feed} \end{cases} \tag{4}$$

$$y_{n+1}V_{n+1} - x_n L_n = \begin{cases} x_D D & \text{above feed} \\ -x_B B & \text{below feed} \end{cases} . \tag{5}$$

On the uppermost tray ($n = 1$) the balance equations simplify to $V_1 = D + L_0$ and $y_1 = x_D$; for the lowest tray ($n = N$, the reboiler) one obtains $L_N = B$ and $x_N = x_B$. For our purposes of looking for optimal diabatic columns, the reflux L_0 is taken equal to zero. Its purpose in an adiabatic column is to help carry heat out of the column. This function is not needed in the diabatic column since heat can be taken directly form tray one.

The temperature dependencies of the molar fractions x and y in the liquid and vapor phase respectively, are given by the state equations for an ideal solution model [13]

$$y = x \exp\left[\frac{\Delta H^{\mathrm{vap},1}(T)}{R}(\frac{1}{T_{\mathrm{b},1}} - \frac{1}{T})\right] \tag{6}$$

$$1 - y = (1 - x) \exp\left[\frac{\Delta H^{\mathrm{vap},2}(T)}{R}(\frac{1}{T_{\mathrm{b},2}} - \frac{1}{T})\right]. \tag{7}$$

$T_{\mathrm{b},1}$ and $T_{\mathrm{b},2}$ denote the boiling points of the two pure components. The enthalpies $\Delta H^{\mathrm{vap},1}(T)$ and $\Delta H^{\mathrm{vap},2}(T)$ are calculated as

$$\Delta H^{\mathrm{vap},i}(T) = \Delta H_b^{\mathrm{vap},i} + (T - T_{\mathrm{b},i})(c_{\mathrm{p}}^{\mathrm{vap},i} - c_{\mathrm{p}}^{\mathrm{liq},i}), \qquad (i = 1, 2) \tag{8}$$

where $\Delta H_b^{\mathrm{vap},i}$ are the heats of vaporization of the pure components and $c_{\mathrm{p}}^{\mathrm{liq},i}$ and $c_{\mathrm{p}}^{\mathrm{vap},i}$ are the corresponding heat capacities. Eq.(8) requires the heat capacities to be temperature independent.

In order to calculate the heat required at each tray to maintain the desired temperature profile, the energy balance has to be maintained for each tray n:

$$Q_n = V_n H_n^{\rm vap} + L_n H_n^{\rm liq} - V_{n+1} H_{n+1}^{\rm vap} - L_{n-1} H_{n-1}^{\rm liq} \,. \tag{9}$$

For conventional adiabatic distillation columns, Eq.(9) would be equal to zero (for $1 \leq n < N$), and there would be no control parameters over which to optimize. The enthalpies $H^{\rm vap}$ and $H^{\rm liq}$ carried by the vapor and liquid flows are determined by

$$\begin{aligned} H^{\rm liq}(T) &= x\, c_{\rm p}^{\rm liq,1}(T - T_{\rm ref}) + (1-x)\, c_{\rm p}^{\rm liq,2}(T - T_{\rm ref}) & (10) \\ H^{\rm vap}(T) &= y \left[c_{\rm p}^{\rm liq,1}(T - T_{\rm ref}) + \Delta H^{\rm vap,1}(T) \right] + \\ &\quad + (1-y) \left[c_{\rm p}^{\rm liq,2}(T - T_{\rm ref}) + \Delta H^{\rm vap,2}(T) \right] & (11) \end{aligned}$$

Here we assumed constant heat capacities, a noninteracting mixture of ideal gases for the vapor phase, and an ideal solution for the liquid phase [13].

For the lowest tray the energy balance reduces to

$$Q_N = V_N H_N^{\rm vap} + B H_N^{\rm liq} - L_{N-1} H_{N-1}^{\rm liq} \,. \tag{12}$$

For condenser and reboiler we obtain

$$\begin{aligned} Q_D &= (D + L_0)(H^{\rm vap}(T_1) - H^{\rm liq}(T_D)) & (13) \\ Q_B &= Q_N \,. & (14) \end{aligned}$$

For diabatic distillation, the reflux $L_0 = 0$ and Eq.(13) becomes

$$Q_D = D(H^{\rm vap}(T_1) - H^{\rm liq}(T_D)) \tag{15}$$

while Eq.(12) assumes the form

$$Q_1 = D H_1^{\rm vap} + L_1 H_1^{\rm liq} - V_2 H_2^{\rm vap}. \tag{16}$$

On the feed tray, the enthalpy of the feed flow has to be considered in Eq.(9):

$$Q_F = Q_n - F H^{\rm liq}(T_F) \,. \tag{17}$$

Note that we assume that the feed enters as liquid at its boiling temperature T_F. The feed tray n is chosen such that the inequality $T_{n-1} < T_F < T_n$ holds.

Eqs.(2)-(17) enable us to evaluate the entropy production of the distillation process. The heat exchange between column and surroundings and the mass flows of distillate, bottoms and feed contribute to the entropy production ΔS^{u}. Since the column is in steady state, its entropy is constant. This implies that the entropy production equals the change in entropy of the column's surroundings. This latter entropy change can be calculated by accounting for all entropy flows into and out of the column. In order to focus on the separation process proper, unobscured by issues of heat exchange, we have chosen to define our system to be the *interior* of the distillation column. This makes the irreversibility associated with heat transfer in and out of the column extraneous to the present optimization[1]. Hence, we take the T_n to be equal to the tray temperatures. We then express the entropy production as

$$\Delta S^{\mathrm{u}} = \sum_{n=0}^{N} \frac{Q_n}{T_n} + \Delta S_{\mathrm{mass\_flows}} \,, \tag{18}$$

where $n = 0$ refers to the condenser. $\Delta S_{\mathrm{mass\_flows}}$ is given by

$$\Delta S_{\mathrm{mass\_flows}} = -F s_F + D s_D + B s_B. \tag{19}$$

The entropies per mole of the mass flows are given by

$$\begin{aligned} s_i &= x_i \left(s_{\mathrm{ref},1} + c_{\mathrm{p}}^{\mathrm{liq},1} \ln \frac{T_i}{T_{\mathrm{ref}}} \right) + (1 - x_i) \left(s_{\mathrm{ref},2} + c_{\mathrm{p}}^{\mathrm{liq},2} \ln \frac{T_i}{T_{\mathrm{ref}}} \right) + \\ &+ R[x_i \ln x_i + (1 - x_i) \ln(1 - x_i)] \,, \qquad (i = F, D, B) \end{aligned} \tag{20}$$

Note that $\Delta S_{\mathrm{mass\_flows}}$ is fixed by the specifications of the process and is therefore not part of the optimization.

3 Equal Thermodynamic Distance

The distillation process is modeled as an N-step process [14], with N corresponding to the number of trays in the distillation column. There is an asymptotice theory bounding the entropy production for such processes in the limit of $N \to \infty$. Asymptotically, the total entropy production ΔS^{u} of

[1] It can be shown that, in the limit of infinite N, the optimization of the column including the entropy production due to heat exchange decouples into two separate problems: the problem considered here and a separate problem of creating a heat exchange network to optimally supply the heats required at each tray.

an N-step process is bounded by $\Delta S^{\rm u} \geq \mathcal{L}^2/(2N)$ (a result from the horse-carrot theorem [4, 5]). The thermodynamic length of an N-step process can be written as

$$\mathcal{L} = \sum_{n=1}^{N} \Delta\mathcal{L}_n \,, \tag{21}$$

where $\Delta\mathcal{L}_n$ is the length of the n-th step. Asymptotically, for minimal entropy production the lengths of the steps have to be equal, i.e.

$$\Delta\mathcal{L}_1 = \ldots = \Delta\mathcal{L}_n = \ldots = \Delta\mathcal{L}_N \,, \tag{22}$$

hence the name, equal thermodynamic distance.

For the distillation model described in the previous section, the thermodynamic length element Eq.(1) is given by [4]

$$d\mathcal{L} = \frac{\sqrt{C_\sigma}}{T}\, dT \,, \tag{23}$$

where C_σ is the total constant pressure coexistance heat capacity of the binary two-phase mixture in equilibrium [15]. This is the heat capacity of a constant pressure system consisting of L moles of liquid coexisting in equilibrium with V moles of vapor. As such a system is heated, the amounts of liquid and vapor change and the compositions readjust in such a fashion as to maintain equilibrium. The quantities of liquid and vapor that need to be counted in C_σ are the flows L and V between trays. To give $V(T)$ and $L(T)$ irrespective of N, these need to be taken equal to the limiting (infinite N) values which are given above the feed by

$$V(T) = \frac{x_D - x(T)}{y(T) - x(T)} D \tag{24}$$

$$L(T) = \frac{x_D - y(T)}{y(T) - x(T)} D, \tag{25}$$

and below the feed by

$$V(T) = \frac{x(T) - x_B}{x(T) - y(T)} B \tag{26}$$

$$L(T) = \frac{y(T) - x_B}{x(T) - y(T)} B. \tag{27}$$

In Figure (3), C_σ of a benzene/toluene mixture is depicted for different purity requirements. In order to establish an ETD path from the condenser

T_0 to the reboiler T_N in a column with N trays, one has to determine temperatures T_n such that

$$\int_{T_n}^{T_{n+1}} \frac{\sqrt{C_\sigma}}{T}\, dT \;=\; \frac{1}{N} \int_{T_0}^{T_N} \frac{\sqrt{C_\sigma}}{T}\, dT\,, \qquad n = 0, \ldots, N-1\,. \tag{28}$$

ETD is a first-order asymptotic theory [4, 5] for minimum entropy production in $\frac{1}{N}$. This gives rise to the question of how reliable is ETD for columns with few trays?

In order to answer this question, we use a fully numerical, multidimensional optimization routine to minimize entropy production for a distillation process and compare this with ETD.

4 Numerical Optimization

Because of its asymptotic nature, the minimum entropy production calculated with ETD will be higher than the true minimum for fewer trays. Consequently, we are interested in the difference between ETD and optimal operation. This motivates our fully numerical optimization, which will find the true minimum for any feasible N.

The entropy production (18), is minimized using a multidimensional optimization routine. Thus, the optimal temperature for each tray in the column is determined; no thermodynamic principle like ETD is applied. Calculating the gradient of Eq.(18) is rather cumbersome due to the structure of the state equations (6)-(7). For this reason, we have chosen Powell's routine [16] to perform the minimizations since it does not require gradient information.

The temperature T_1 at the uppermost tray as well as the temperature T_N at the reboiler are fixed by the given distillate and bottoms purity requirements x_D and x_B respectively. This reduces the number of control variables to $N-2$. For convenience, in the following description, we will use $M = N-2$ for the number of variables. The minimization algorithm consists of the following steps:

1. An initial temperature profile $\vec{\mathbf{T}}_0 = (T_1, \ldots, T_N)$ for the N trays with the temperatures being sorted, i.e. $T_1 < T_2 < \ldots < T_{N-1} < T_N$, and an initial set of search directions $(\vec{\mathbf{u}}_1, \ldots, \vec{\mathbf{u}}_M)$ are given. Usually, the $\vec{\mathbf{u}}_i$ are the standard basis vectors of $\mathcal{R}^M$.

2. Repeat the following procedure until the entropy production stops decreasing:

   - For each direction $\vec{\mathbf{u}}_i$, $i = 1, \ldots, M$, minimize along that direction using the temperature profile $\vec{\mathbf{T}}_{i-1}$ as starting point. Save the result as $\vec{\mathbf{T}}_i$. The line minimization is performed by a bracketing routine and parabolic interpolation (Brent's method [17, 16]). Save direction $\vec{\mathbf{u}}_L$ along which the entropy production made its largest decrease Σ. Save the average direction moved $\vec{\mathbf{T}}_M - \vec{\mathbf{T}}_0$.
   - Using the objective function $\Delta S^{\mathrm{u}}(\vec{\mathbf{T}})$, define the quantities

$$\xi_0 \equiv \Delta S^{\mathrm{u}}(\vec{\mathbf{T}}_0), \quad \xi_N \equiv \Delta S^{\mathrm{u}}(\vec{\mathbf{T}}_M), \quad \xi_E \equiv \Delta S^{\mathrm{u}}(2\vec{\mathbf{T}}_M - \vec{\mathbf{T}}_0)\,. \tag{29}$$

   - If one of the inequalities

$$\xi_E \geq \xi_0 \quad \text{or} \quad \frac{2(\xi_0 - 2\xi_M + \xi_E)[(\xi_0 - \xi_M) - \Sigma)]}{\Sigma(\xi_0 - \xi_E)^2} \geq 1, \tag{30}$$

     holds, then keep the old direction set. Save $\vec{\mathbf{T}}_M$ as $\vec{\mathbf{T}}_0$. Go back for another iteration. If condition (30) does not apply, discard the direction of largest decrease $\vec{\mathbf{u}}_L$ and assign $\vec{\mathbf{u}}_L \leftarrow \vec{\mathbf{u}}_M$. This avoids a buildup of linear dependence of the search directions. Assign $\vec{\mathbf{u}}_M \leftarrow (\vec{\mathbf{T}}_M - \vec{\mathbf{T}}_0)$. Minimize along the new $\vec{\mathbf{u}}_M$ and save the result as $\vec{\mathbf{T}}_0$. Go back for another iteration.

However, one problem may arise using the algorithm above. The entropy production (18) consists of terms of the form Q_n/T_n which in turn are functions of the liquid and vapor flows V_n and L_n. An explicit representation of the vapor flow above the feed using the material balance (4) and (5) is given by

$$V_n(T_n, T_{n-1}) = \frac{x_D - x_{n-1}(T_{n-1})}{y_n(T_n) - x_{n-1}(T_{n-1})} D\,. \tag{31}$$

Analogous expressions exist for the liquid flows and the trays below the feed. Eq.(31) has a singularity, the flow becomes infinite for $y_n = x_{n-1}$. This leads to an undesired instability of the optimization algorithm: At the beginning of a line minimization along a particular search direction the minimum needs to be bracketed. Otherwise, the one-dimensional minimization routine may identify this singularity as the minimum and lead to an unphysical result, e.g. a large negative value for the entropy production.

For a few trays, the ETD steps to cover the total distance L are unphysically large, requiring a higher concentration of the more volatile component in the liquid of the tray above than enters as the vapor from the tray below (see figure 7). This requires a higher than infinite reflux flow rate which the equations manage by making some of the flow rates negative. It is somewhat surprising that the numerical optimization also has difficulty here. The reason is linked to the high heat demand on these trays, which diverges as we approach infinite reflux. The vertical asymptotes lead to numerical instabilities which will be explored in future studies.

As initial guesses we used linear temperature profiles in all our optimizations. In general, minimum entropy production was obtained after a few N iterations using a relative accuracy of 10^{-9}.

5 Results and Discussion

For our comparison of the entropy production associated with distillation on shorter (small N) columns, we chose benzene/toluene as our system to be separated. The entropy production for the separation of a 50/50 mole fraction benzene/toluene mixture is minimized by applying both methods. The number of trays and purity requirements are varied to show differences in the performance of ETD and numerical optimization. The comparisons are always between columns with the same material flows in and out. Notably the feed, bottoms and distillate flows match not only in magnitude but also in composition and temperature in the columns compared.

The results for the simulations are shown in figures 4, 5 and 6. The figures show the entropy production as a function of the number of trays for (i) a conventional column (ii) the ETD column, (iii) the numerically optimized column, and (iv) the asymptotic lower bound ($\mathcal{L}^2/2N$) for the entropy production based on the ETD calculation.

The $\mathcal{L}^2/2N$ values are suprisingly far from the ETD curves. The reason for this comes from the fact that the flow rates V and L enter the expression for C_σ. The values of V and L are the continuous values given in equation (23) which corresponds to an infinite number of trays. The continuous path is needed to define thermodynamic distance along the column. When the temperatures found from equation (28) are used to calculate the actual flow rates with the given number of trays N, the flow rates are significantly above

the minimum reflux levels and account for the difference[2]. The surprisingly good match between $\Delta S^u_{optimal}$ and ΔS^u_{ETD} led to a deeper explanation. It turns out that the match between these two quantities is always order $1/N^3$ [18].

For all three purity requirements the optimal columns were far more efficient than their conventional adiabatic counterparts. The optimal results also were above the ETD lower bound, but approached the ETD bound as N was increased. The large N simulation for the 99/01 purity requirement had the closest values to the ETD bound as was expected due to the asymptotic nature of the ETD theory. The numerical optimization results predicted slightly less entropy production in the small N regions, but agreed very well with the ETD results for larger N values. Sample temperature and heating profiles for the three different systems are also shown.

The temperature profiles (figures 8, 9 and 10) for both methods have the characterisic mild 'S' curvature found in optimally operating columns where the separation is symmetric. This shape of the temperature profiles is probably due to the effective heat capacity C_σ. The temperature difference from tray to tray in the column is smaller in the regions where the heat capacity is large. As can be seen in figure (3), the 99/01 separation is the most dramatic example of this.

The heating profiles (figures 11, 12 and 13), show the largest differences between the two methods studied here. The figures show that in general the ETD column requires larger condensers and reboilers than the optimal column but smaller heat exchangers on intermediate trays. Since squeezing large heat exchangers into distillation trays has proved to be a difficult task, this may be a desirable feature for some installations. Another thing to note is that the heat demands for the intermediate trays are fairly small and roughly the same for all the trays. On closer examination, of the heat demand for the 71 tray column, we note that the demands near the feed and near the reboiler and condenser are significantly higher than the demands on the trays in between. This gives the familiar (inverted-u)-u shape shown in figure 14 previously noted in other studies [5, 19, 6, 7]. A similar examination of the 15 tray column shows only a slight tendency toward this behavior and keeps $|Q_n| \approx$ constant for $1 < n < N$. Nearly constant heat demand makes Rivero's

[2]This reflux rate refers to the value of $V - L$ for that plate and should not be confused with the reflux rate L_0 for the column which is needed to be non-zero for the conventional column but is zero for the ETD and the optimal columns.

design for diabatic columns quite attractive [8]. His design employs two heat exchangers: one above and one below the feed. Each heat exchanger winds its way through the column and this arrangement can probably approximate the optimal heating / cooling profiles we find.

6 Conclusion

In the present manuscript we compared the entropy production for ETD operation and numerically optimized operation of a distillation column. The calculations assumed reversible heat transfer and equilibrium stages on each tray. Similar studies comparing a different optimization algorithm to an isoforce criterion have appeared elsewhere [9, 10, 11].

For columns with many trays the agreement between ETD and optimal operation is good. More surprisingly, the agreement between the entropy productions is remarkably good even for moderate length columns. For shorter columns there are significant deviations, particularly in the heating profiles. The optimal profile calls for a nearly constant heat demand which works well with the Rivero implementation of diabatic columns [8].

References

[1] Sieniutycz S., Salamon P. (Eds.), Finite-Time Thermodynamics and Thermoeconomics, Advances in Thermodynamics 4, Taylor and Francis, New York, 1990.

[2] Hoffmann K.H., Burzler J.M., Schubert S., Endoreversible thermodynamics, J. Non-Equilib. Thermodyn., 22 (1997), 311-355.

[3] Z.Fonyo.: "Thermodynamic Analysis of Rectification I and II. Reversible Model of Rectification, Finite Cascade Models",", Int. Chemical Engng., 14, (1) 18 (1974), and 14, (2) 203 (1974).

[4] Salamon P., Nulton J.D., The geometry of separation processes: A horse-carrot theorem for steady flow processes, Europhys. Lett., 42 (1998), 571-576.

[5] Andresen B., Salamon P., Optimal distillation using thermodynamic geometry, in: Thermodynamics of Energy Conversion and Transport, Sieniutycz S., De Vos A. (Eds.), Springer, New York, 2000.

[6] E. Sauar, G. Siragusa, and B. Andresen. Equal thermodynamic distance and equipartition of forces principles applied to binary distillation. to appear, Journal of Physical Chemistry.

[7] G.M. de Koeijer, S. Kjelstrup, G, Siragusa, P Salamon, M. Schaller, and K.H. Hoffmann. Comparison of Entropy Production Rate Minimization Methods for Binary Diabatic Tray Distillation. Proceedings of ECOS01, ed. A. Ozturk (2001).

[8] R. Rivero. L'analyse d'exergie: Application à la Distillation et aux Pompes à Chaleur à Absorption. PhdThesis, Institut National Polytechnique de Lorraine, Nancy, France 1993.

[9] S. Kjelstrup-Ratkje, E. Sauar, E. Hansen, K. M. Lien, and B. Hafskjold. Analysis of entropy production rates for design of distillation columns". Ind. Eng. Chem. Res. 34 (1995) 3001-3007.

[10] E. Sauar, R. Rivero, S. Kjelstrup, and K. M. Lien. Diabatic column optimization compared to isoforce columns. Energy Convers. Mgmt. 38 (1997) 1777-1783.

[11] G.M. de Koeijer, S. Kjelstrup, H.J. van der Kooi, B. Groß, K.F. Knoche, and T.R. Andersen. Positioning Heat Exchangers in Binary Tray Distillation Using Isoforce Operation. Proceedings of ECOS99, ed. M. Ishida, Tokyo ISBN4-9980762-0-5 (1999) 471-476.

[12] King C.J., Separation Processes, McGraw-Hill, New York, 1971.

[13] Lewis G.N., Randall M., Thermodynamics, McGraw-Hill, New York, 1961.

[14] Nulton J.D., Salamon P., Andresen B., Anmin Q., Quasistatic processes as step equilibrations, J. Chem. Phys., 83 (1985), 334-338.

[15] J.S. Rowlinson, Liquids and Liquid Mixtures, Plenum Press, New York, 1969.

[16] Press W.H., Numerical recipes in C, Cambridge University Press, 1992.

[17] R.P. Brent, Algorithms for Minimization without Derivatives, Prentice-Hall, Englewood Cliffs (NJ), 1973.

[18] J.D. Nulton and P. Salamon. Optimality in Multi-stage Operations with Asymptotically Vanishing Cost. submitted to SIAM Journal of Control and Optimization

[19] Danielle Brown. Simulations of Equal Thermodynamic Distance Distillation Columns for Regular Solutions. MS Thesis, Applied Mathematics, San Diego State University, 1998.

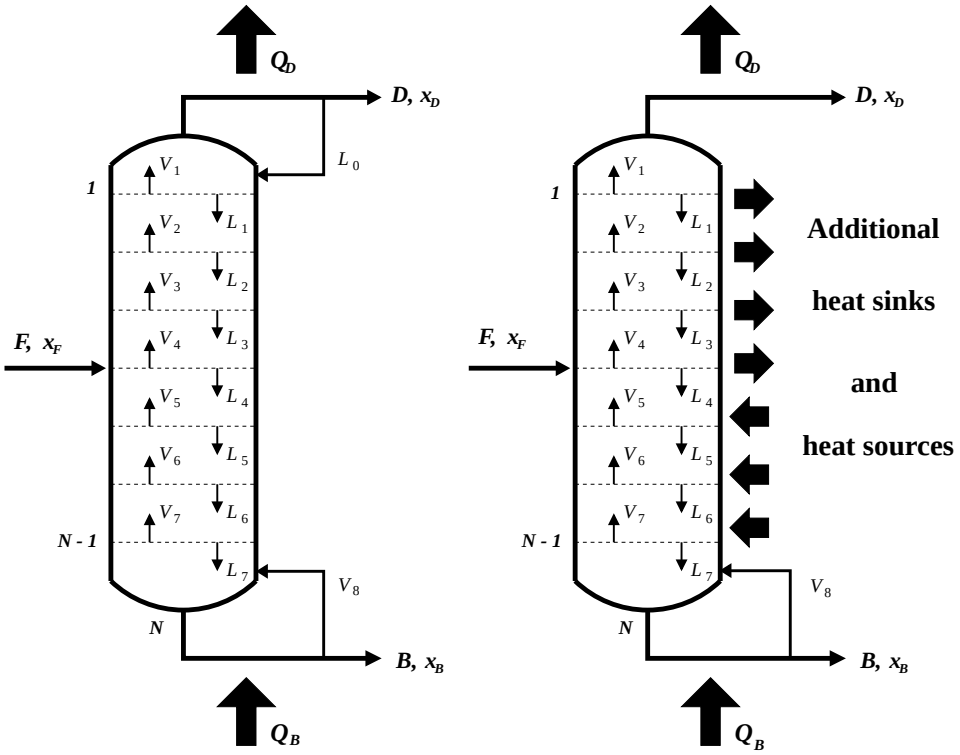

Figure 1: Sketch of a conventional adiabatic distillation column and a diabatic column with additional heat exchange. Both columns have $N = 8$ trays including the reboiler as tray 8.

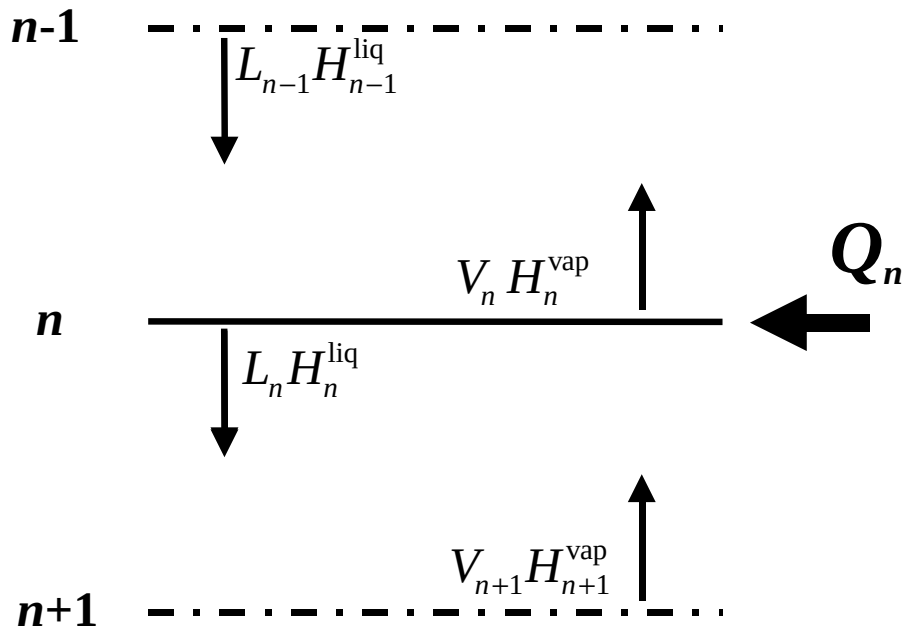

Figure 2: Definition of quantities around tray n appearing in the balance equations (4), (5) and (9).

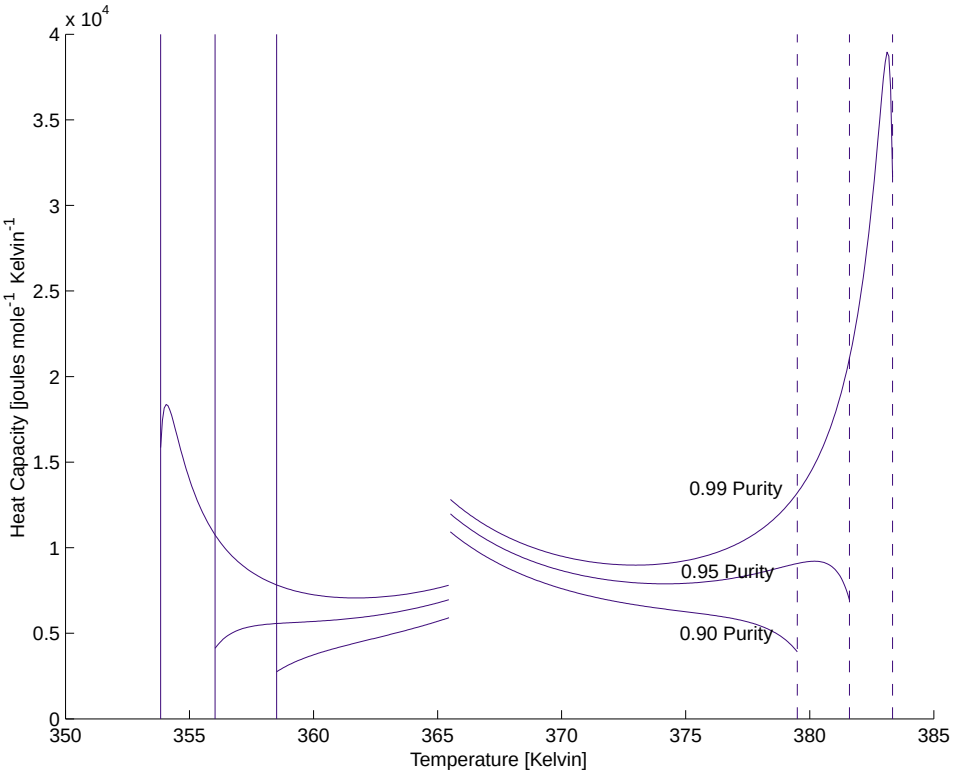

Figure 3: Heat capacity C_σ in equation (23) as a function of temperature for three different purity requirements ($x_D/x_B = 0.9/0.1$, $0.95/0.05$, $0.99/0.01$). The break at 366 K corresponds to the feed point.

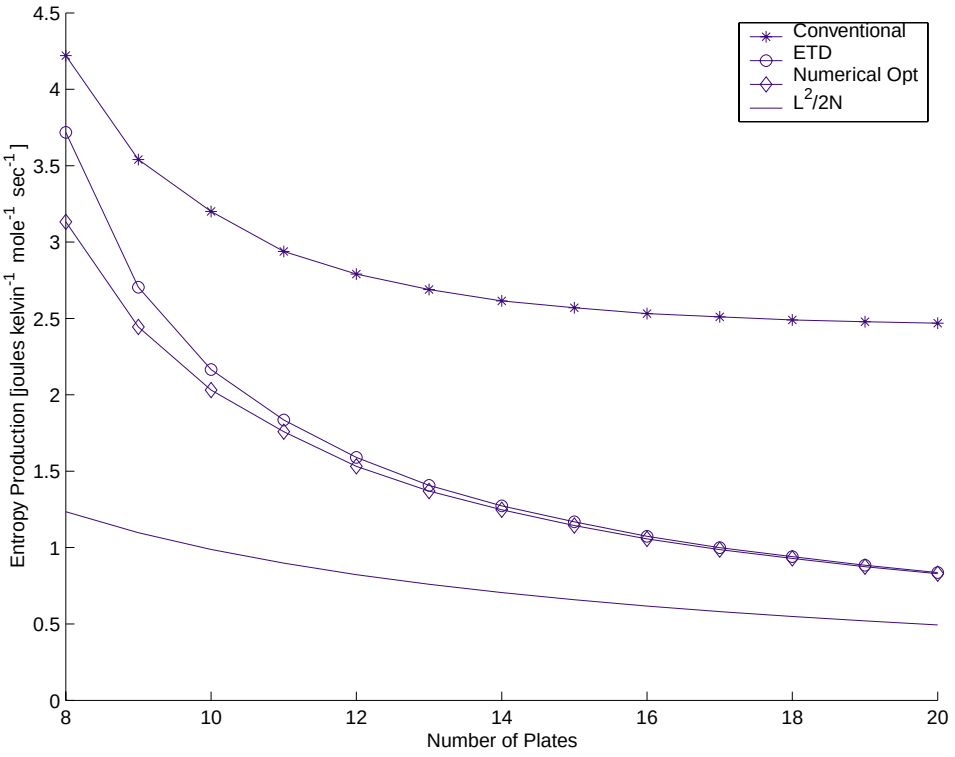

Figure 4: Minimal entropy production for varying numer of trays determined with ETD and numerical optimization. The purity requirement is $x_D = 0.9$, $x_B = 0.1$. For comparison, the entropy production for a conventional column (CC) and the lower bound for ETD, $L^2/(2N)$, is included.

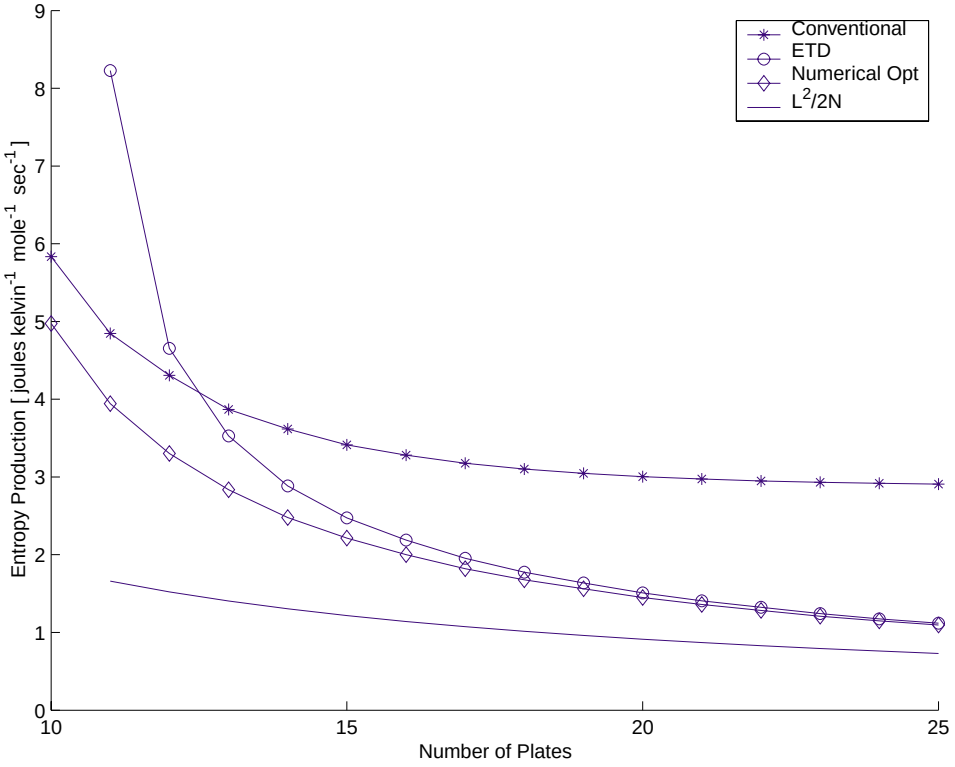

Figure 5: Entropy production for purity requirement $x_D = 0.95$, $x_B = 0.05$.

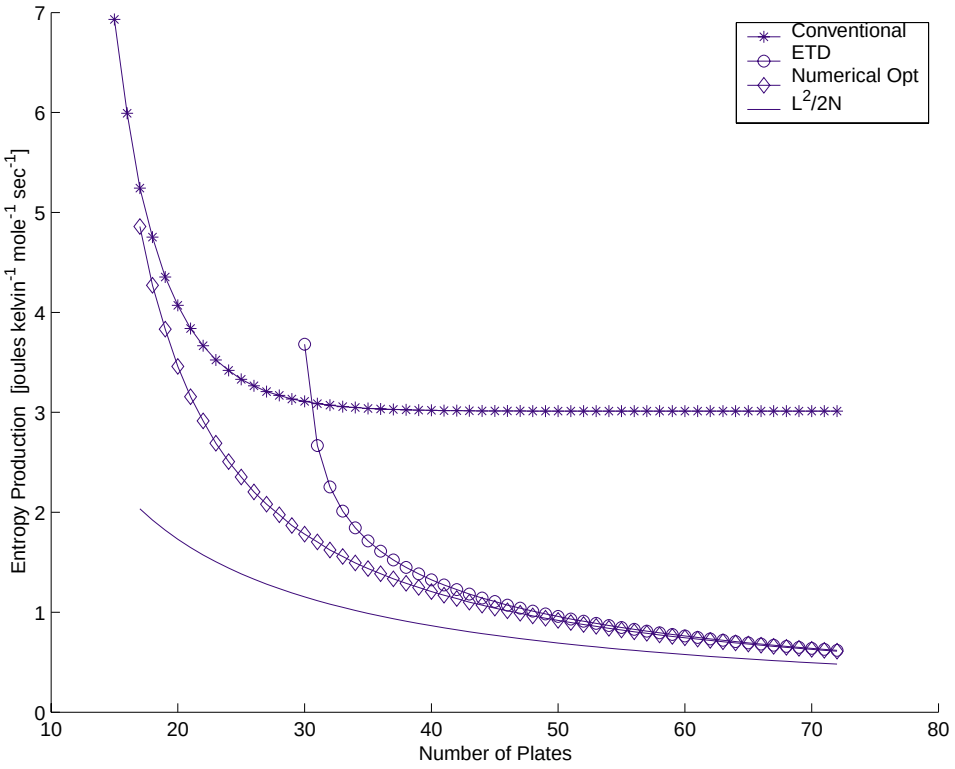

Figure 6: Entropy production for purity requirement $x_D = 0.99$, $x_B = 0.01$.

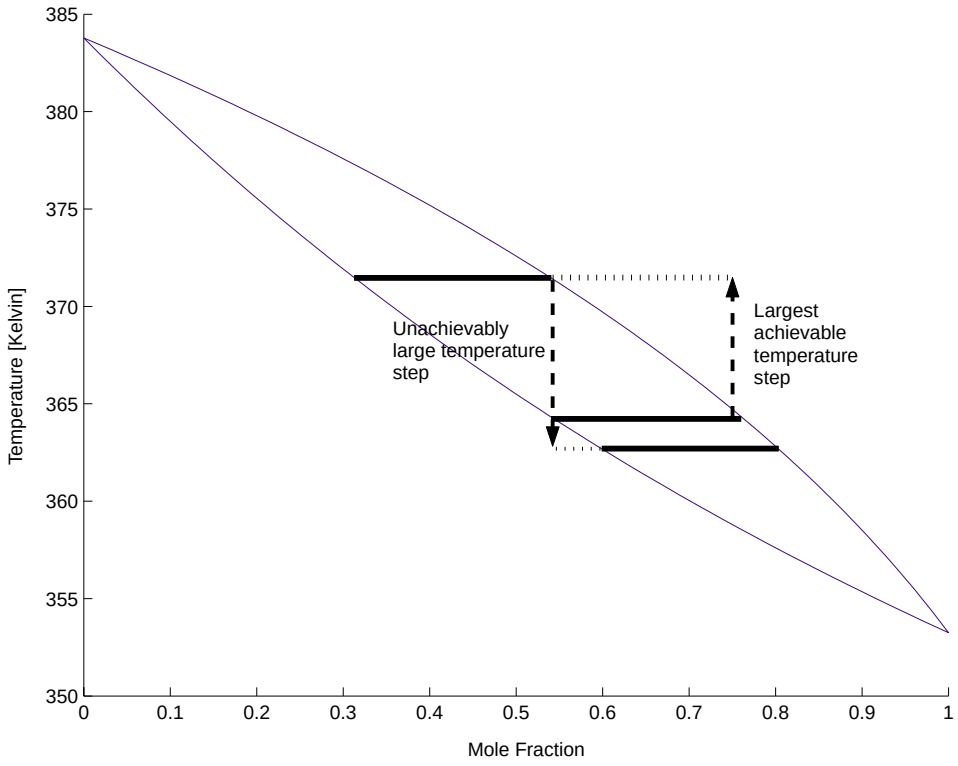

Figure 7: Description of an unphysical situation in the vapor-liquid-diagram

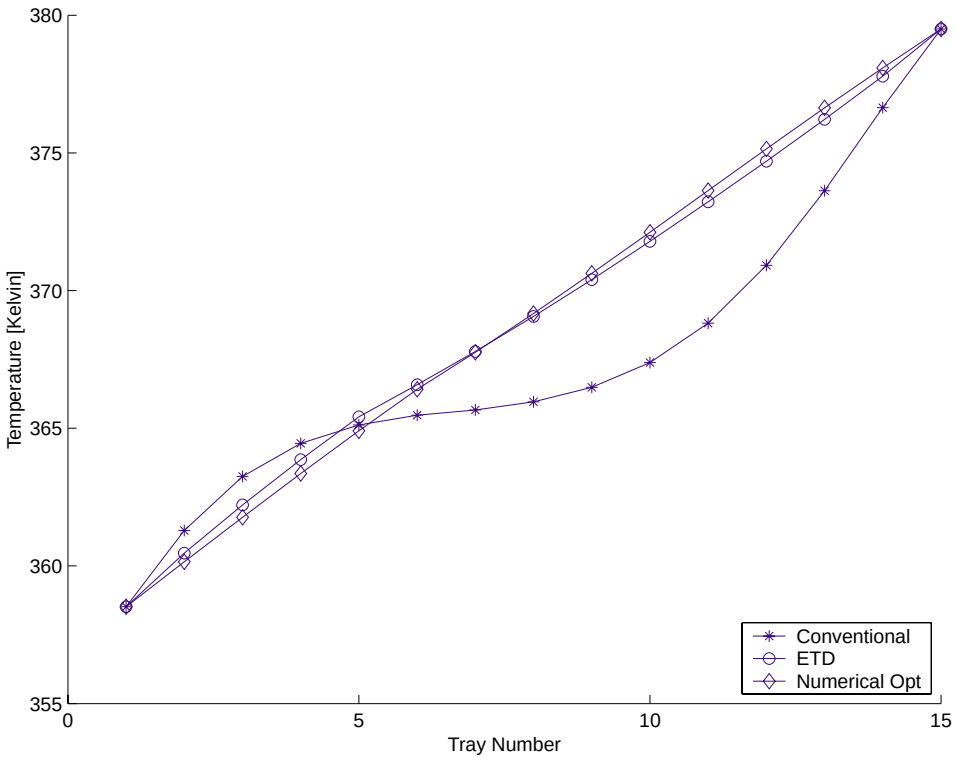

Figure 8: Optimal temperature profile for a 15 tray column (purity requirement $x_D = 0.9$, $x_B = 0.1$)

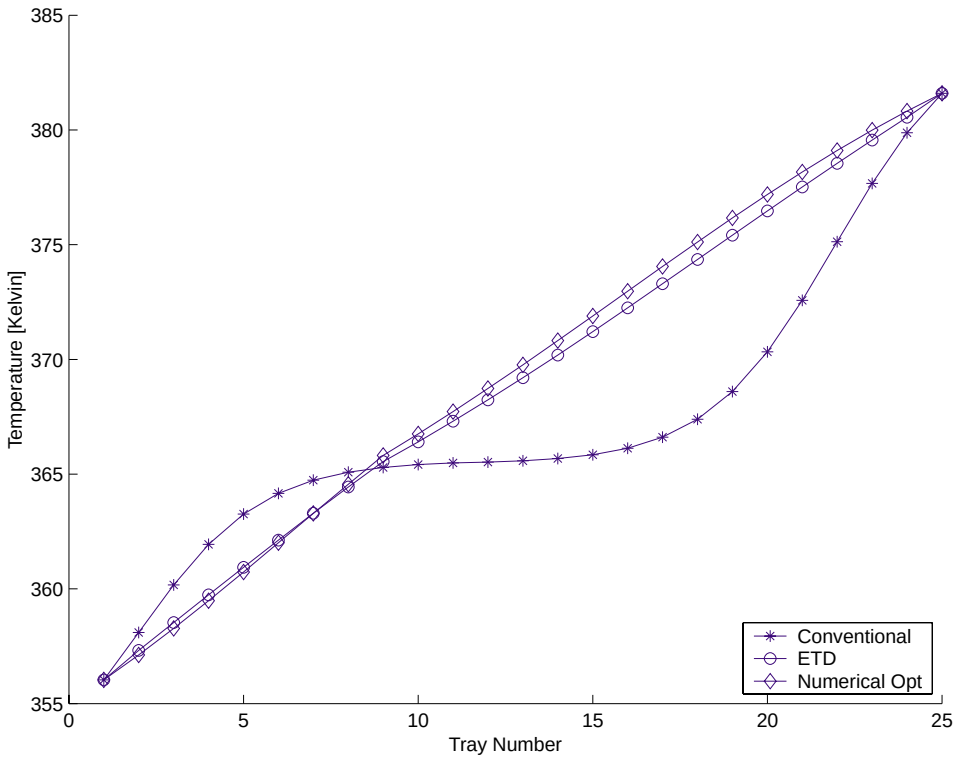

Figure 9: Optimal temperature profile for a 25 tray column (purity requirement $x_D = 0.95$, $x_B = 0.05$)

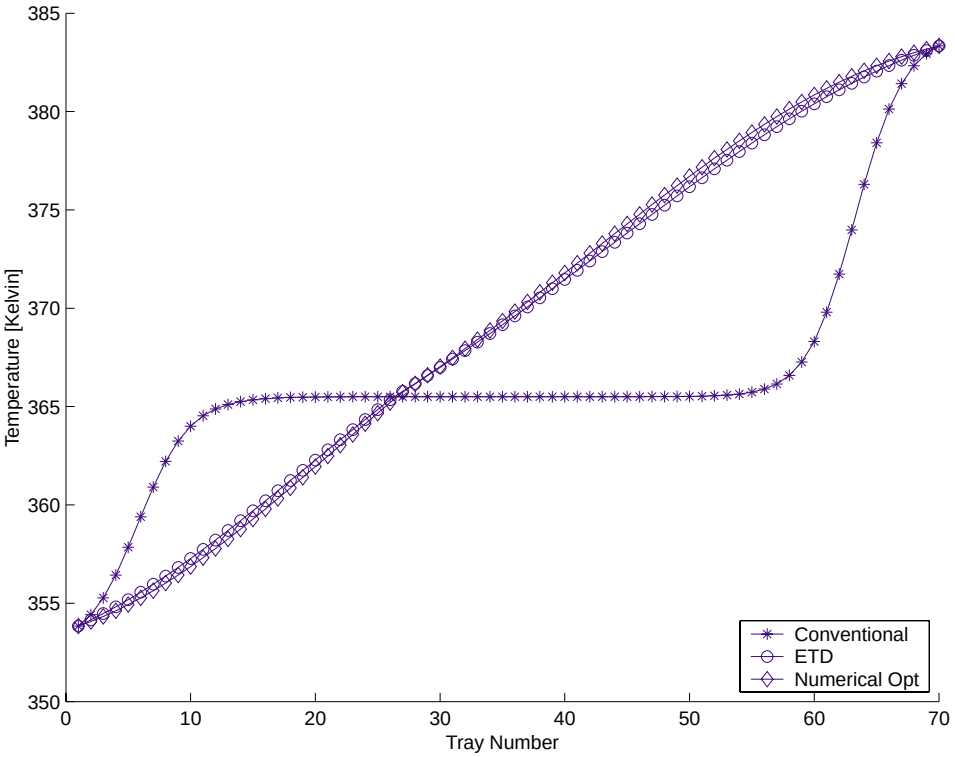

Figure 10: Optimal temperature profile for a 70 tray column (purity requirement $x_D = 0.99$, $x_B = 0.01$)

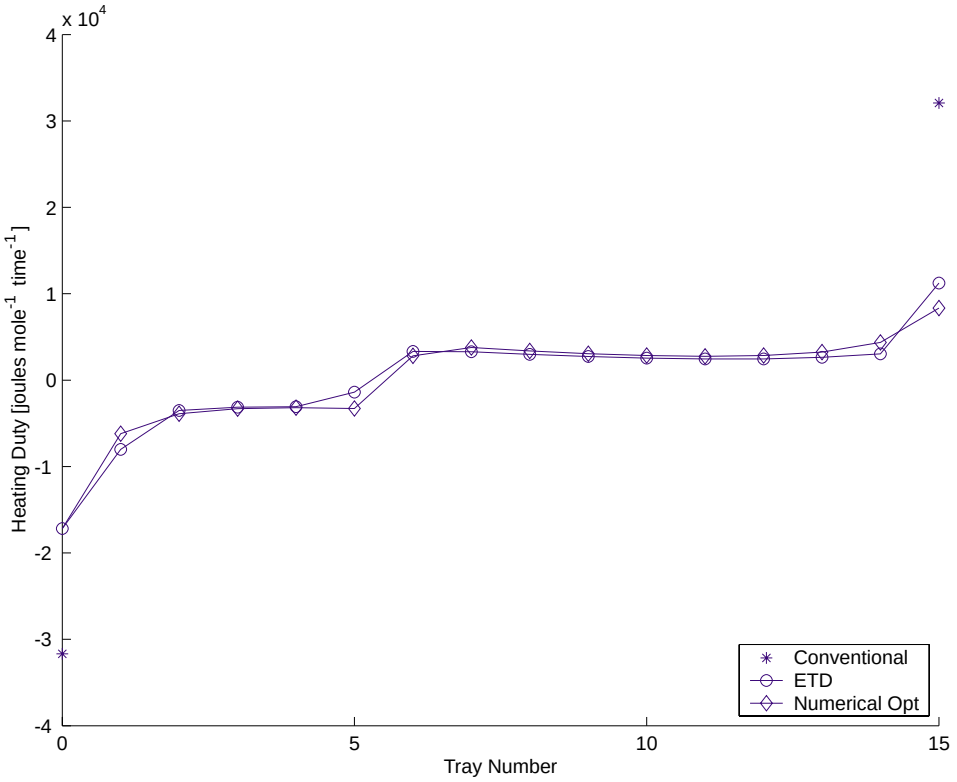

Figure 11: Corresponding heating requirements for a 15 tray column (purity requirement $x_D = 0.9$, $x_B = 0.1$)

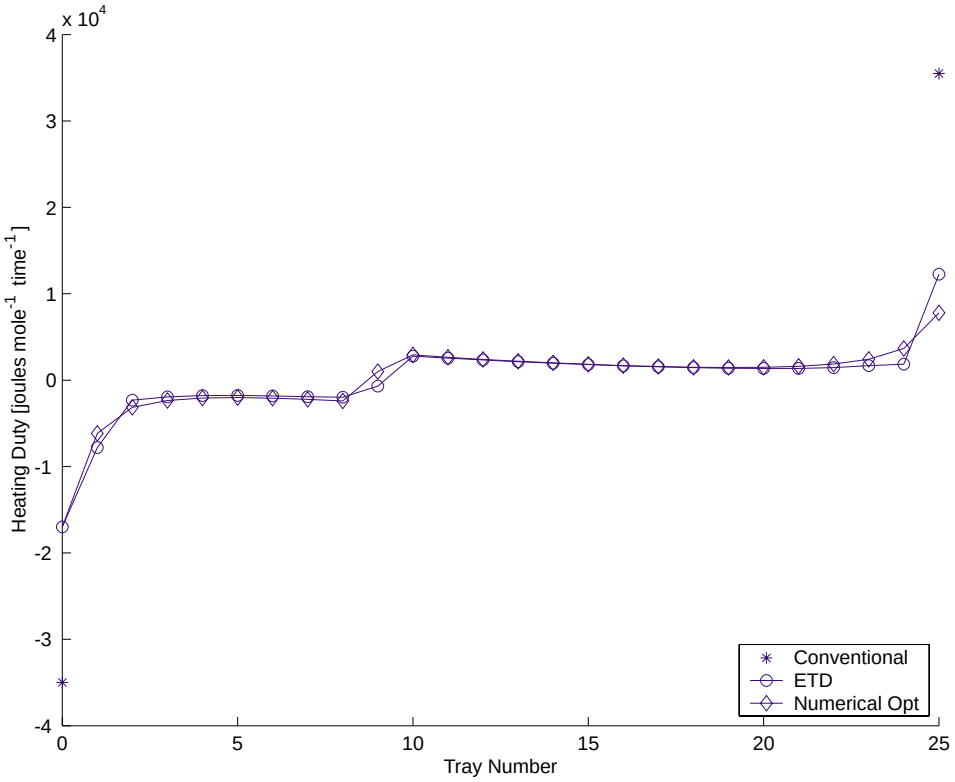

Figure 12: Corresponding heating requirements for a 25 tray column (purity requirement $x_D = 0.95$, $x_B = 0.05$)

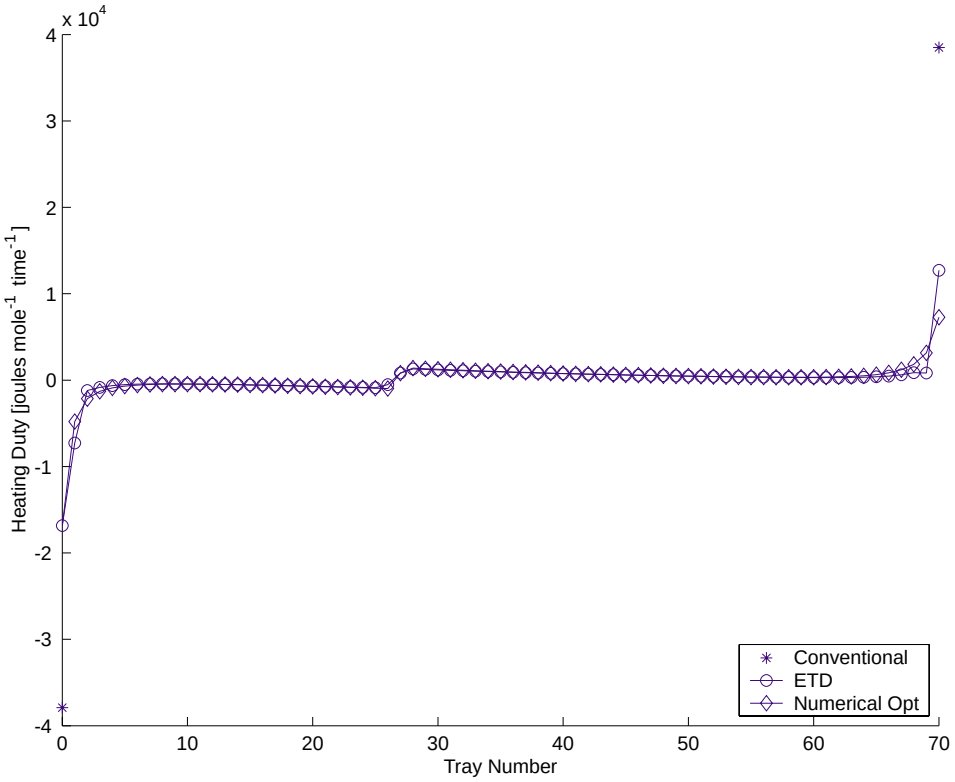

Figure 13: Corresponding heating requirements for a 70 tray column (purity requirement $x_D = 0.99$, $x_B = 0.01$)

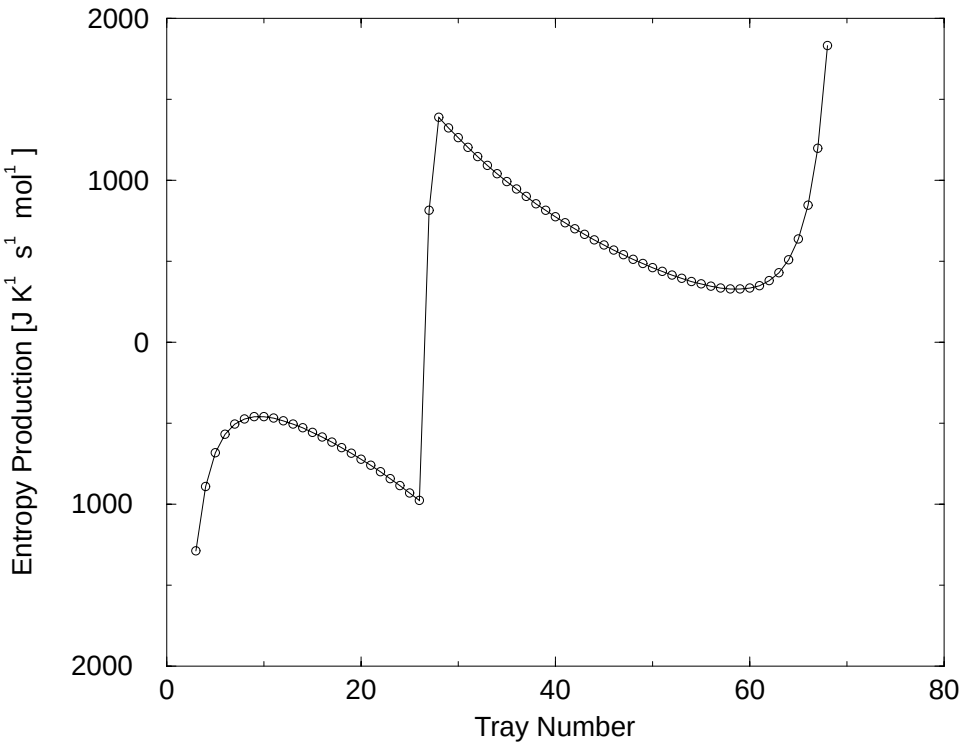

Figure 14: The familiar (inverted u) - u shape of the optimal heating profile. Data shown is the same as in figure 13 with end trays omitted.